

# Aspects of MLS Measuring Systems\*

JOHN VANDERKOOY\*\*, AES Fellow

*Department of Physics, University of Waterloo, Waterloo, Ont., N2L 3G1, Canada*

A maximum-length sequence (MLS) has mathematical properties that make it very useful as an excitation signal for measurement in audio and acoustics. The pathology of MLS systems when there is distortion of various kinds is explored. The resulting artifacts can falsify a reverberation plot, reduce the distortion immunity of the measurement system, and give rise to spurious reflections in the impulse response, to name a few negative aspects. On the other hand, MLS systems can also allow the determination of the total distortion of an electroacoustic system when excited by a signal of any desired spectrum, and sensitive tests for determining the presence of distortion are possible due to the time-domain separation of linear and nonlinear components.

## 0 INTRODUCTION

Any excitation signal that is spectrally dense, that is, a signal that has energy at all frequencies in its intended range of operation, can be used as a test signal for a general-purpose measurement system. Pulses, chirps, and binary maximum-length sequences (MLS) are thus all good candidates for such signals. With some computer manipulation almost any signal can be synthesized repeatably and used in an instrument. In addition, a measuring system may employ a periodic stimulus of any of the types mentioned, and the system under test may be properly measured if its response dies away adequately in one period. With control from a general-purpose computer, relatively simple sampled-data systems are possible which use a variety of these techniques.

Swept or stepped tones have been used for many decades, and chirps having frequency proportional to time with tracking delayed bandpass filters have been pioneered by Heyser [1] to measure the full complex transfer function. Fully computer-controlled time-delay spectrometry (TDS) instruments have existed for some

time. In modern instruments based on this technique [2] the accuracy can be very high, and Poletti [3], [4] has shown how the system response can be completely recovered from measurements made at any sweep rate, a process hinted at in a reply to comments on a related paper by the author [5], [6].

The use of pulses was pioneered by Berman and Fincham [7], [8], who with fast Fourier transform (FFT) techniques were able to achieve high signal-to-noise ratios in spite of the common belief that pulses have a poor signal energy. In fact a pulse of very high amplitude can be applied to a loudspeaker system to determine its impulse response. The distortion during such a short pulse is somewhat irrelevant, serving only perhaps to renormalize the excitation level, since the total mechanical energy imparted to the driver is manageable, and the resulting impulse response is unaffected by distortion.

For room acoustic impulse responses, a very long decay must be measured, and an excitation signal must also have high energy to counteract acoustic noise and quantization error in the analog-to-digital converter. For these reasons, MLS signals were used by Schroeder [9] and others [10], [11], and a more detailed analysis of MLS techniques was carried out by the author and the designer of the first commercially available MLS system analyzer [12]. There are a number of reasons that MLS techniques are so apt for room acoustics, the

\* Presented at the 93rd Convention of the Audio Engineering Society, San Francisco, CA, 1992 October 1–4; revised 1994 February 4.

\*\* Member of the Guelph–Waterloo Program for Graduate Work in Physics [(GWP)<sup>2</sup>].

most cogent being the ease of generation of a suitable-length signal of high energy by simple shift-register circuits, the application of efficient algorithms to provide a long impulse response, and the immunity to noise and distortion of such systems. MLS systems are now popular for many system-identification tasks, perhaps because the excitation signal has good crest factor, is more pleasing to listen to (or endure), and excites systems more naturally.

The author has a personal, perhaps irrational, preference for MLS systems, and has used one over the years, developing a feeling for the system with its strengths and occasional weaknesses. Any system must be used with intelligence and the wisdom gained by experience, or otherwise false conclusions can easily be drawn. In this paper the author wishes to analyze some of the pathology of MLS systems, so that others will not as easily be misled, and also to propose some ideas allowing the peculiarities of such systems to be used to advantage.

## 1 REVIEW OF MLS MEASUREMENTS

When applied as an excitation, the periodic MLS signal consisting of 1s and 0s from a shift register is transformed to a bipolar signal of amplitude  $\pm V_0$ . This signal has length  $L = 2^m - 1$  samples, where  $m$  is the order of the shift register. Usually 1 relates to  $-V_0$  and 0 to  $+V_0$ . This allows the *exclusive-OR* truth table to be considered as a simple multiplication. The MLS signal is normally applied with a zero-order hold function, and this introduces a  $(\sin f)/f$  error, as in any such sampled-data system. We will assume that the relevant correction has been applied in any case and not consider this aspect further.

If  $x(n)$  represents the sequence of +1s and -1s, the signal applied to the device under test (DUT) is  $V_0x(n)$ , and the periodic output  $y(n)$  will be

$$\begin{aligned} y(n) &= V_0x(n) * h(n) \\ &= V_0 \sum_{k=-\infty}^{\infty} x(k)h(n-k) \end{aligned} \quad (1)$$

where  $*$  denotes linear convolution and  $h(n)$  is the impulse response of the DUT. The circular autocorrelation of the MLS has the property

$$\begin{aligned} C(n) &= \frac{1}{L+1} \sum_{k=0}^{L-1} x(k)x(n+k) \\ &= \delta(n) - \frac{1}{L+1} \end{aligned} \quad (2)$$

where all indices are calculated mod  $L$ . Except for a small dc shift, the autocorrelation function is a periodic unit sample or impulse.

The circular cross correlation  $z(n)$  of  $x(n)$  with  $y(n)$ ,

normalized by the amplitude  $V_0$ , leads to [12]

$$\begin{aligned} z(n) &= \frac{1}{L+1} \sum_{k=0}^{L-1} x(k) \frac{y(n+k)}{V_0} \\ &= \frac{1}{L+1} \sum_{k=0}^{L-1} \sum_{l=-\infty}^{\infty} x(k)x(n+k-l)h(l) \\ &= \sum_{l=-\infty}^{\infty} h(l) \frac{1}{L+1} \sum_{k=0}^{L-1} x(k)x(k+n-l) \\ &= \sum_{m=-\infty}^{\infty} \sum_{l=0}^{L-1} h(l+mL) \left[ \delta(n-l) - \frac{1}{L+1} \right] \\ &= \sum_{m=-\infty}^{\infty} h(n+mL) - \frac{1}{L+1} \sum_{m=-\infty}^{\infty} h(m) \end{aligned} \quad (3)$$

Thus except for a small inconsequential dc term,  $z(n)$  is essentially the impulse response of the system, but it is periodic and wrapped on a length  $L$ . For a proper measurement,  $L$  must be long enough that  $h(n)$  has decayed sufficiently in one period, or else there is time aliasing. If the DUT has no response at dc, then the last term is zero anyway, and most MLS analyzers neglect it. We call  $z(n)$  the periodic impulse response (PIR), and loosely we think of it as the normal impulse response when the MLS measurement has been properly made.

In calculating the impulse response in an MLS system, it is tempting to make the correction for the small dc shift that is seen in the preceding equations and also discussed by Borish and Angell [11, eq. 20]. However, when there is even-order distortion, significant dc offsets can occur, and the correction gives a resulting PIR which shows a strong unnatural offset that deviates from the typical expected linear behavior. Hence the correction should not be applied, even if the system has response at dc.

## 2 DISTORTION IN MLS MEASUREMENTS

In an earlier paper [12], it was argued that the effects of distortion in the DUT were spread more or less uniformly throughout the PIR by virtue of the complexity of the intermodulation products in weakly nonlinear cases. An MLS of length  $L$  samples and sampling rate  $f_s$  contains all frequencies from  $f_s/L$  to  $(1 - 1/L)f_s/2$  with frequency separation  $f_s/L$ , all with equal amplitude. It seems reasonable to expect a nonlinearity such as a quadratic or cubic component to result in a confused jumble of intermodulation products of all kinds which would alias to other frequencies, such that the net effect would almost be an added noise. The author had noticed for some time that some loudspeakers when driven hard showed a strange lumpiness in the impulse response.

It was decided to investigate by computer simulation the effects of a host of different types of nonlinearity, including simple quadratic and cubic memoryless distortion.

An interesting study by Dunn and Hawksford [13] has appeared which shows that in some situations errors due to nonlinearity are unevenly distributed in the MLS measurement period, and this prevents the expected reduction of errors by zeroing a portion of the impulse response of longer MLS measurements. Their results agree with the author's findings for simple distortion, but it is shown later that most other forms of distortion show very uniform distribution of errors. Slew distortion, however, gives rise to an extremely uneven distribution of errors. In fact much of the error forms a coherent spike that can be very obfuscating in analyzing an impulse response.

To assess the effects of distortion, real measurements could have been used, but in order to control well the nature and amount of the distortion, computer simulations were substituted. Such simulations can then be a guide as to the type of distortion actually present in a real measurement. An MLS of various lengths was generated by the computer, a common choice being a sequence of length 4095 resulting from a 12th-order shift register. This sequence could be convolved with any model impulse response, or a real measured response, to generate the MLS-excited signal of an equivalent truly linear system. At this point various forms of distortion can be applied to the signal, and the contaminated impulse response can be obtained from these modified data by a cross correlation with the original MLS. All calculations are done single-precision floating point, and thus have a relative error as low as  $2^{-24}$  (−144 dB).

The distortion component alone can be used in the cross correlation, thus displaying more clearly the artifacts in the resulting error, since the cross-correlation algorithm is associative with respect to the behavior of distorted and undistorted components.

An important aspect of an MLS is the effective probability density function (PDF) of the excitation which ultimately creates the distortion. An unfiltered MLS is a binary signal, having very high slew rates, and it would not excite a system in a normal fashion. Thus low-pass filtering is usually employed, and the PDF becomes spread out. An MLS with more terms in its characteristic polynomial (that is, more feedback taps) generally has less skewing of the PDF when it is low-pass filtered [14]. It makes sense to apportion a significant amount of the antialiasing filter to the MLS excitation signal, since this results in nearly Gaussian PDF. This ensures that the distortion in the DUT will be sampled at many levels. Many systems, of course, have their own scarifying effect on the PDF, but it is wisest not to trust this to produce acceptable PDFs. Another way to alter the two-valued nature of the MLS signal is to pass it through one or several all-pass filters. The effect of the filter can be removed by normalization to determine the proper system frequency response.

### 3 LOW-ORDER DISTORTION

A normal electrodynamic driver has various nonlinearities of low order. The strength of the field in the gap has a linear and a quadratic dependence with displacement along the gap, resulting in second- and third-order distortion. The suspension often stiffens with travel, and this produces third-order distortion. The static magnetic field is somewhat modulated by the current in the voice coil, creating another form of second-order distortion. Hence it is useful to study the effects of such distortion with simulations.

To scale the distortion in a consistent way, the rms level of the output signal  $y_{\text{rms}}$  of an undistorted system is used as a reference. To define  $m^{\text{th}}$ -order distortion, for example, an undistorted signal  $y(n)$  will be modified by a relative distortion  $a$  to a signal  $d(n)$  given by

$$d(n) = y(n) + a \frac{[y(n)]^m}{y_{\text{rms}}^{m-1}}. \quad (4)$$

Fig. 1 shows the near-field impulse response of an electrodynamic driver unit measured under two signal levels—2 V rms [Fig. 1(a) and (b)] and 20 V rms [Fig. 1(c) and (d)]. The vertical and horizontal scales are chosen to show both the early response and the late-time portion of interest. It is clear that at higher signal level there are localized artifacts in the impulse response, which are spread more or less randomly, as well as a noiselike component. A 4095-point MLS was used. We shall assume that the lower level measurement is correct, and use that impulse response in our simulations. Fig. 1(e) is the frequency response associated with the high-level data of Fig. 1(c) and (d). The “noise” in the response is a result of the distortion.

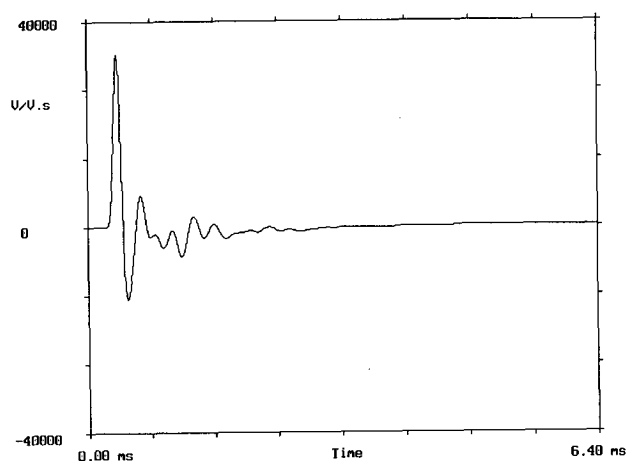
The impulse response of Fig. 1(a) was convolved with the same 4095-point MLS used in the measurement, having feedback taps at shift register positions 12, 11, 10, and 2. This signal is shown in Fig. 2(a), and its rms level is 1.16 V. Second-order distortion [ $m = 2$  in Eq. (4)] with  $a = 0.1$  was added to this signal, and the resulting impulse response after cross correlation is shown in Fig. 2(b). Fig. 2(c) shows the cross correlation of only the second-order distortion component, which is somewhat irregular and not very uniformly spread. Fig. 2(d) shows the resulting impulse response after applying third-harmonic distortion with  $a = +0.1$ , and Fig. 2(e) and (f) shows on different scales the cross correlation of only the distortion component. Two points are salient—the distortion artifacts for the third-harmonic distortion are more numerous and more uniformly spread, and there is a large component having exactly the same shape as the original linear-only impulse response.

This latter component represents essentially a gain change in the system, and it occurs for all odd-order forms of distortion. Even-order distortion creates a dc bias and asymmetry in a signal. The dc bias is often not directly seen due to the ac coupling of most signals.

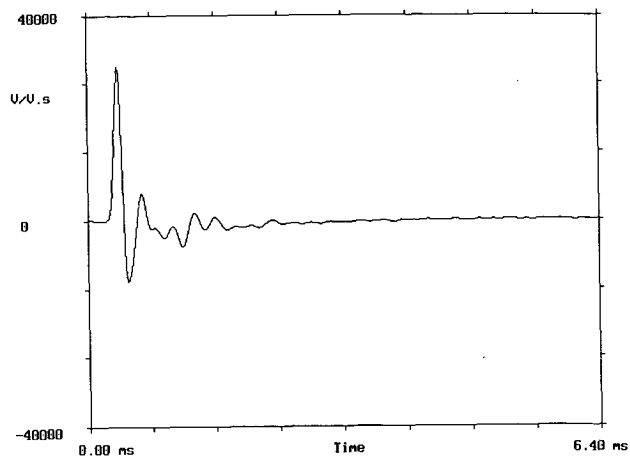
For negative  $a$  values, third-order distortion simulates reasonably well a system that is approaching saturation. It is intuitively obvious that odd-order distortion will renormalize the gain of a system, and a general theory of this aspect is now presented.

Let us assume that a frequency-independent or memoryless transfer characteristic is applicable, so that the output signal  $y$  is related to the input signal  $x$  by

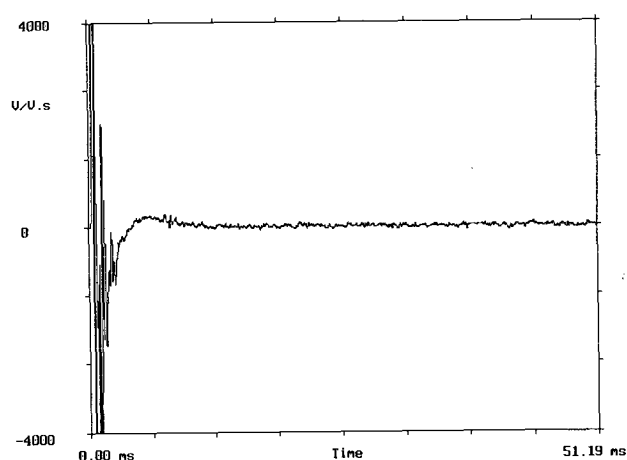
$$y = f(x) \quad (5)$$



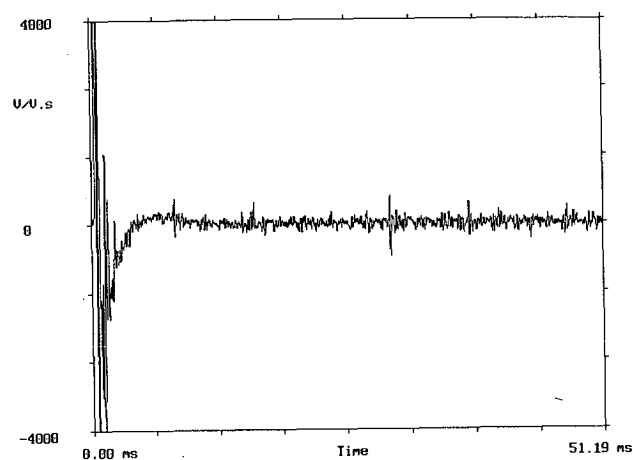
(a)



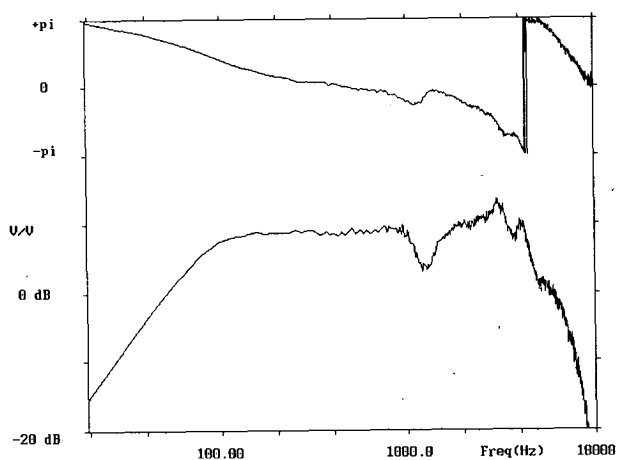
(c)



(b)



(d)



(e)

Fig. 1. Near-field MLS measurement of 100-mm low-frequency driver unit in sealed box. (a), (b) Impulse response on different vertical and horizontal scales to display both initial transient and longer time behavior. Sampling frequency was 80 kHz and a 4095-point MLS was used, low-pass filtered at 10 kHz, with an excitation level of 2 V rms. (c), (d) Same measurements made at a level of 20 V rms. Distortion artifacts are clearly visible in (d) and result in frequency response shown in (e).

and the function  $f(x)$  will contain both linear and higher order distortion terms. There may be frequency dependences both before or after the memoryless stage, so there is not too much loss of generality. We assume

that the signal  $x$  driving the nonlinearity in Eq. (4) has a PDF given by  $p(x)$  and has zero mean.

To calculate the effective linear gain  $G_1$  of a system with nonlinearities as described by Eq. (5), we can

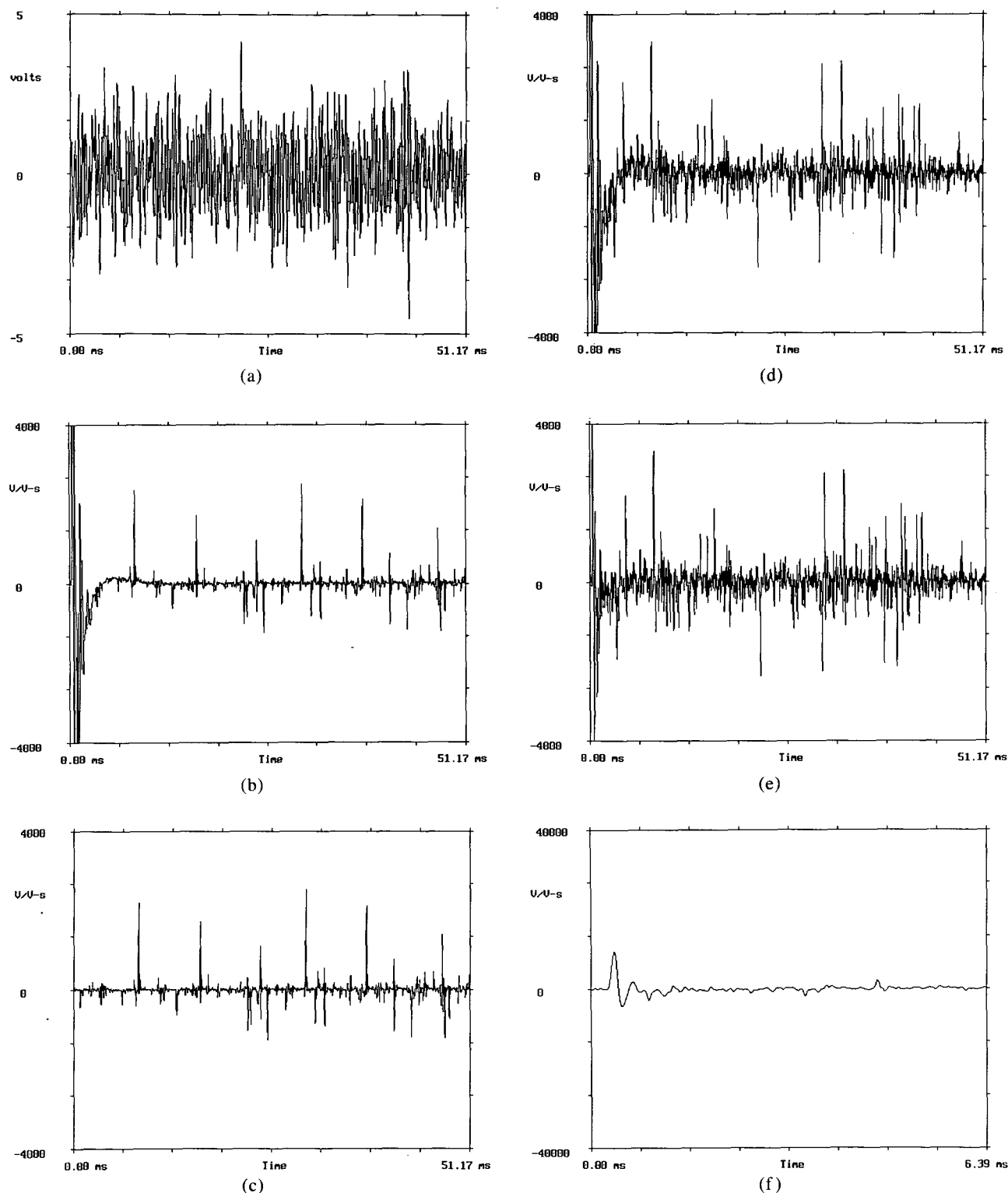


Fig. 2. Series of simulations of distortion in MLS measurements, using as starting point low-level data of Fig. 1. (a) Microphone signal of undistorted data before cross correlation. (b) Cross-correlated PIR when second-order distortion with  $a = 0.1$  (see text) is added. (c) Effect of distortion component only. (d), (e) Counterparts of (b), (c) for addition of third-order distortion. (f) Different view of (e), showing that distortion contains image of original impulse response (a), hence changing system gain. (g) Plot of distortion component of PIR for second-order distortion, but for different MLS of same order. It should be compared with (c), showing that positions of artifacts are peculiar to sequence used.

model the system by the linear component

$$y_l = G_l x + K \quad (6)$$

where  $K$  is a constant. If we then demand that the time-averaged mean-square error  $E$  between  $y_l$  and  $y$ , given by

$$E = \int_{-\infty}^{\infty} [G_l x + K - f(x)]^2 p(x) dx \quad (7)$$

is minimized by setting  $\partial E / \partial G_l = 0$ , the linear gain can be shown to be given by

$$\begin{aligned} G_l &= \frac{\int_{-\infty}^{\infty} x f(x) p(x) dx}{\int_{-\infty}^{\infty} x^2 p(x) dx} \\ &= \frac{1}{x_{\text{rms}}^2} \int_{-\infty}^{\infty} x f(x) p(x) dx \end{aligned} \quad (8)$$

An example using Eq. (8) can be calculated to show the reasonableness of this approach. If, for example, the transfer characteristic is

$$f(x) = bx + \frac{kx^3}{x_{\text{rms}}^2} \quad (9)$$

and a sinusoidal excitation  $x = x_0 \cos \omega t$  is used which has a PDF proportional to  $1/[1 - (x/x_0)^2]^{1/2}$ , then we can show that the linear gain  $G_l = b + 3k/2$ , which is exactly what we would expect for this system by substituting  $x = x_0 \cos \omega t$  in Eq. (9) and calculating the amplitude of the  $\cos \omega t$  component.

A filtered MLS will have a more Gaussian PDF given by

$$p(x) = \frac{1}{\sqrt{2\pi} x_{\text{rms}}} \exp\left(-\frac{x^2}{2x_{\text{rms}}^2}\right) \quad (10)$$

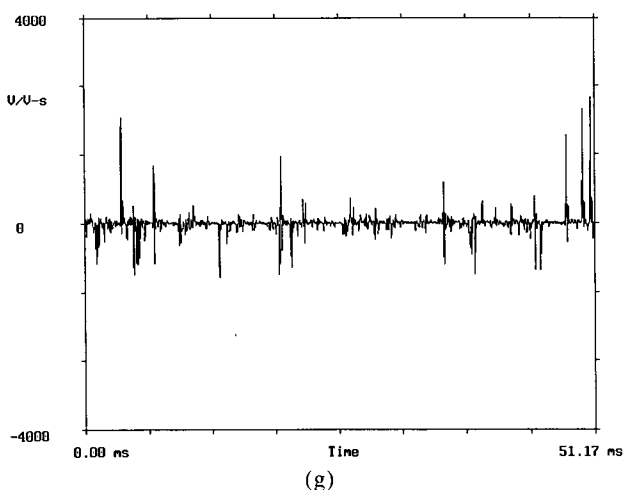


Fig. 2. continued

and this leads to an effective gain of  $b + 3k$ . The PDF of the output signal  $y$  will not be Gaussian, and both the linear and the nonlinear signal components change. If we model the transfer characteristic as

$$y = f(x) = bx + f_{\text{nl}}(x) \quad (11)$$

in which the function  $f_{\text{nl}}(x)$  deals with the nonlinear part and  $G_{\text{nl}}$  is the gain change from  $b$  due to nonlinearity, then we can write

$$f(x) = (b + G_{\text{nl}})x + [f_{\text{nl}}(x) - G_{\text{nl}}x] \quad (12)$$

where the term in square brackets represents the nonlinear-only part, with all linearities removed.

The total linear MLS energy  $E_l$  will be

$$E_l = (b + G_{\text{nl}})^2 x_{\text{rms}}^2 \quad (13)$$

while the nonlinear energy (spread presumably throughout the PIR) will be

$$E_{\text{nl}} = \int_{-\infty}^{\infty} [f_{\text{nl}}(x) - G_{\text{nl}}x]^2 p(x) dx, \quad (14)$$

the statistical second moment of the nonlinear-only component.

As a check on some of these concepts, we return to the data of Fig. 1(a), which shows the impulse response of the undistorted system, and Fig. 2(f), which shows the PIR of third-order distortion with  $a = +0.1$  as given by Eq. (4). The PDF is reasonably Gaussian in this example, and thus we expect the distortion to change the gain by a fraction  $3a = 0.3$ , or 30%. The strength of the image in Fig. 2(f) is 28.5% of that in Fig. 1(a), so there is good agreement. We could if desired also compute the total linear and nonlinear energy.

Our example is a bit simplistic in that a memoryless distortion was applied, whereas in reality the distortion may be frequency dependent. Thus we cannot simply apply the ideas here to analyze a particular situation. In fact, from the data it is not feasible to work out the type and level of the distortion in each case. We must content ourselves with changes in gain and estimates of total distortion energy.

We can also try to analyze the data in Fig. 1(c), taken with a high signal level. The main peak is down about 10% from the data in Fig. 1(a), and the total distortion is about 7%, as determined by summing the energy in all the artifacts. The nature of the artifacts is not quite like second-order distortion [Fig. 2(b) and (c)] nor quite like third-order distortion [Fig. 2(d), (e), and (f)] but specific peaks can be identified, especially by comparing with the second-order simulation. The remaining distortion artifacts in Fig. 1(d) are more noiselike and may not relate to low-order distortion. The 10% reduction of the peak in the PIR may be partly due to the effect of a saturating odd-order nonlinearity, but it is perhaps also partly due to voice-coil heating which reduces the sensitivity of the driver. It is also possible that the time-varying aspects of this heating are re-

sponsible for some of the noiselike components of the distortion in the PIR. This aspect is discussed later.

Turning back to the distortion artifacts, we see that low-order distortion results in components in the MLS-deconvolved PIR that do not have the temporal structure of noise, but rather an irregular impulsive behavior for a broad-band weakly nonlinear DUT. This distortion has a fixed pattern for a specific DUT and MLS. If the 12th-order MLS used is changed to one having feedback taps at 12, 7, 4, and 3, then the distortion artifacts for second-order distortion look like Fig. 2(g). This should be compared with Fig. 2(c) and shows that the details of the distortion are like a fingerprint, being intimately associated with a particular MLS. There are in fact 144 cyclically distinct MLSs of order 12 [15], and so in principle the distortion could be largely identified and removed by using different MLSs and comparing the associated PIRs.

The irregular temporal character of low-order distortion in MLS measurements harms the immunity to distortion of such systems, and this point has been

studied in some detail [13]. The spectrum of the distortion is wider than that of the linear component in narrow-band systems, but the temporal shape of the distortion artifacts is similar to that of the linear component of the PIR.

Distortion of loudspeakers can influence the measurement of the decay of reverberation in room acoustics. The reverberation decay is usually obtained from the impulse response  $h(t)$  measured in a room, by using the reverse integration of  $h^2(t)$ , as shown by Schroeder [9]. Low-order distortion contaminates the PIR, and the resulting Schroeder plots show deleterious effects. Fig. 3(a) shows the impulse response of a loudspeaker-microphone combination in a normal laboratory room, with a large signal level of 20 V rms to the loudspeaker. The PIR shows extraneous "noise" and irregular behavior at times for which the response should be decaying smoothly. Fig. 3(b) shows the unfiltered Schroeder plot, and it is clear that the decay is stunted by the wide-band distortion noise and the irregular low-frequency signal. The wide-band noise is

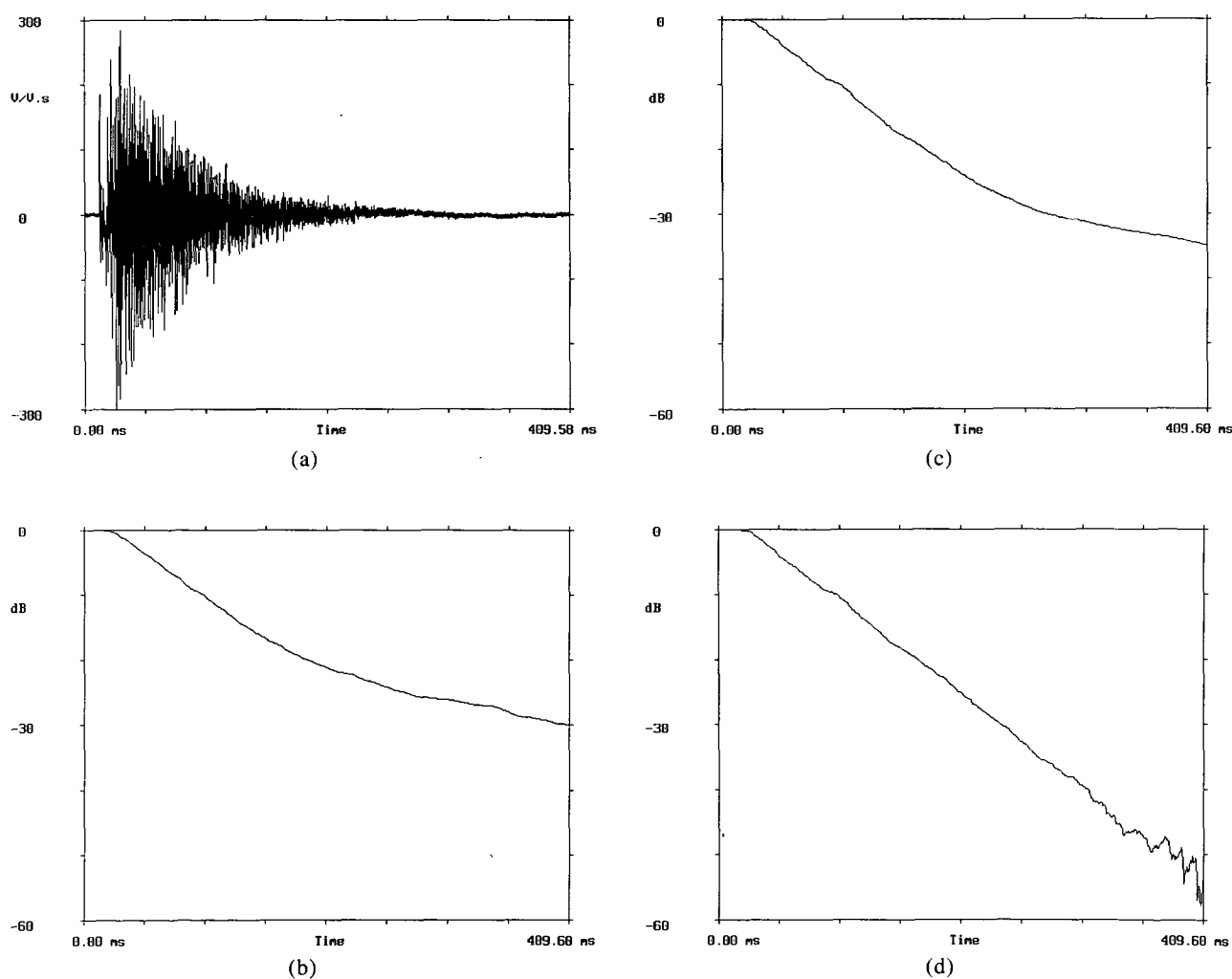


Fig. 3. Series of plots showing effect of distortion on Schroeder plot to determine reverberation time. (a) Measured 16383-point room impulse response of our laboratory with 20 V rms of signal fed to normal loudspeaker. There is some extra "noise" due to distortion, as well as some low-frequency room noise. (b) Wide-band Schroeder plot, displaying saturation due to the noise. (c) 3-kHz one-octave-filtered Schroeder plot which removes effect of low-frequency noise but still suffers from effects of distortion. (d) Effect of compensating for noise and subtracting it out to produce a better decay plot.

a result of distortion in the loudspeaker, but the low frequencies come from ventilation noise in the building. When the impulse response is octave bandpass filtered at 3 kHz, the Schroeder plot looks like Fig. 3(c), and we see that the decay is better but still somewhat stunted by noise.

If the distortion is noiselike and uniform, then the plot can be compensated in the following manner. From the early decay, which is reasonably accurate, one can extrapolate and find a late portion of the PIR which is nearly all distortion or noise. The average energy of this noise can then be determined, and its energy (assuming incoherent addition) can be subtracted while producing the reverse integration of the plot. The resulting plot will then decay to much lower levels before showing the effects of the remaining noise. Fig. 3(d) shows the effect of this procedure. It is clearly beneficial, and the starting decibel value of the plot can also be chosen to give roughly a straight overall tail. The author has used such a procedure for some time to counteract noise and distortion, and it is usually best to use operator intervention to adjust the parameters of the compensation. However, wise experimenters will attempt to make such measurements better by reducing the relative effects of noise. Fans and other sources of noise should be shut off if possible. There is clearly an optimum signal level, since too high a signal level will provoke distortion, which acts in much the same way as noise in reducing the dynamic range of a reverberation plot. If a loudspeaker displays irregular artifacts in the PIR when there is distortion, as shown, for example, in Fig. 1(d), then the Schroeder plot will be adversely affected toward later times, making the plot rough and steplike.

#### 4 TIME-VARYING SYSTEMS

An MLS measurement is predicated on the idea that the transfer function under study is not a function of time. We discuss here what happens when a slow gain change occurs during the measurement, and focus on considerations such as time jitter in the sampling of the MLS data, or time variations of the system itself. Examples are slow heating of a loudspeaker voice coil, speed fluctuations of a tape recorder, air currents in a room, and noise in trigger or sampling circuits. We will show that most of these effects cause a uniformly spread noiselike random fluctuation in the PIR.

Suppose that we are measuring a room's impulse response with an MLS period sufficiently long that some system parameter changes during the measurement. A simple example is the heating up of a voice coil in a loudspeaker as power is applied to it from a voltage-source power amplifier. As the wire heats, the resistance rises, and the current falls, thus changing the system gain (and perhaps the damping and hence the response as well). Using a current-source amplifier is one solution to such a problem, but not a common one, for a number of reasons such as uncontrolled damping, open-circuit instability, and so on.

Let us model the phenomenon by a slow linear gain change over the MLS period, assuming that the gain falls by a small fraction  $\beta$ , as shown in Fig. 4(a). We will regard the MLS signal to be deconvolved as consisting of two components, one a constant one of relative level  $1 - \beta/2$ , the other a bowtielike component of relative level  $\beta/2$  at the ends, but tapering linearly to zero in the middle and reversing phase for the tapering up of the second half. Fig. 4(b) shows this component for the same system described in the low-order distortion section, using  $\beta = 0.2$ .

The first constant MLS signal of relative level  $1 - \beta/2$  will result in a PIR that is reduced slightly in amplitude by the factor  $1 - \beta/2$ , while the bowtie portion will be badly scrambled by the cross correlation, resulting in essentially uniformly spread noise. Fig. 4(c) shows the MLS deconvolved result of the bowtie component of Fig. 4(b), and we see that the result is uniform and noiselike, having none of the characteristics of the system PIR of Fig. 1(a). It is easily shown that if the MLS signal is modeled as constant noise, the  $\beta/2$  amplitude bowtie modulation will result in an MLS component of rms amplitude  $\beta/(2\sqrt{3})$ , giving a noiselike PIR component of this relative level. If the system gain, for example, is reduced by 1% during an MLS period, the signal-to-noise ratio will be limited to  $200\sqrt{3}$  in amplitude, or approximately 51 dB. A Schroeder plot derived from such data would not decay below this level without compensation for the noiselike PIR component.

The spectrum of the bowtie component is similar to that of the linear component, since the gain variation is gentle and hence there is little local change in the time variation, but over longer times there is significant change and even phase reversal. We might expect some of the very lowest frequencies to show significant spectral change.

A model of time jitter effects can be formulated as follows. Suppose that  $\tau(n)$  represents the time jitter at sample  $n$ , and that we know  $[df/dt](n)$ , the slope of the MLS data at each nonjittered sample interval. Then the approximate error at each time sample is simply  $\tau(n) \cdot [df/dt](n)$ . If we know the statistics of the jitter, we can use the jittered samples  $f_j(n)$  to give an estimate of the statistics of the derivative  $[df/dt](n)$ , and hence estimate the error. A computer simulation using the system whose PIR is presented in Fig. 1(a) shows that a white uniform-PDF time jitter of half a time sample peak to peak creates an approximately white contaminating signal which restricts the signal-to-noise ratio to 28 dB.

If one considers measurements of long PIRs in rooms for the purpose of determining reverberation time or the modulation transfer function (MTF), will the ventilation-induced motion of the air in the room cause jitter via Doppler shifts or breakup of acoustic wavefronts so that errors occur? We are not quite sure, since the measured data in the tail of the PIR in reverberant surroundings seem to be somewhat different from measurement to measurement, yet the derived reverberation



time remains consistent. It seems likely that although the data in the tail of the PIR represent sound that has been multiply reflected, for example, the ensuing irregularity in the exact placement of the energy is not important for the extraction of the important acoustic parameters. However, the effective noise levels may be slightly higher due to the jitter. Better controlled experiments on this aspect still need to be done.

## 5 OTHER TRANSFER CHARACTERISTIC ABERRATIONS

Nonlinearities such as crossover distortion, clipping, gain changes at the origin, slew limiting, and other pathology all have significant consequences in MLS measurements.

Crossover distortion results in the addition to the MLS signal of a series of error pulses related to the zero crossings of the waveform, the direction, and possibly the slope. In general this causes an irregular error component to the PIR which may not be uniformly spread, and whose spectrum is usually fairly white in computer simulation. Clipping is similar in character,

but is a much stronger function of level, as one might expect.

A gain change depending on the instantaneous polarity of a signal can be decomposed into a small linear gain change with a symmetrical cusp nonlinearity at the origin, resulting in even-order distortion. Simulation shows that this effect is not uniformly spread, and it is similar to second-order distortion.

Slew limiting may occur especially in power amplifiers when driven with an MLS signal having little filtering. The sharp logic edges of the MLS shift register output have very large slopes, and hence slewing may occur. Such errors may or may not be symmetrical, that is, having the same magnitude of error for negative or positive transitions. Symmetrical slewing distortion of an MLS represents effectively a derivative of the sequence, so that the occurrence of such slewing will add a portion of doublet (derivative of the unit pulse function) to the cross correlation, which represents a component rising with frequency. This response error will propagate through to the final PIR upon cross correlation, but other more interesting effects can occur as well.

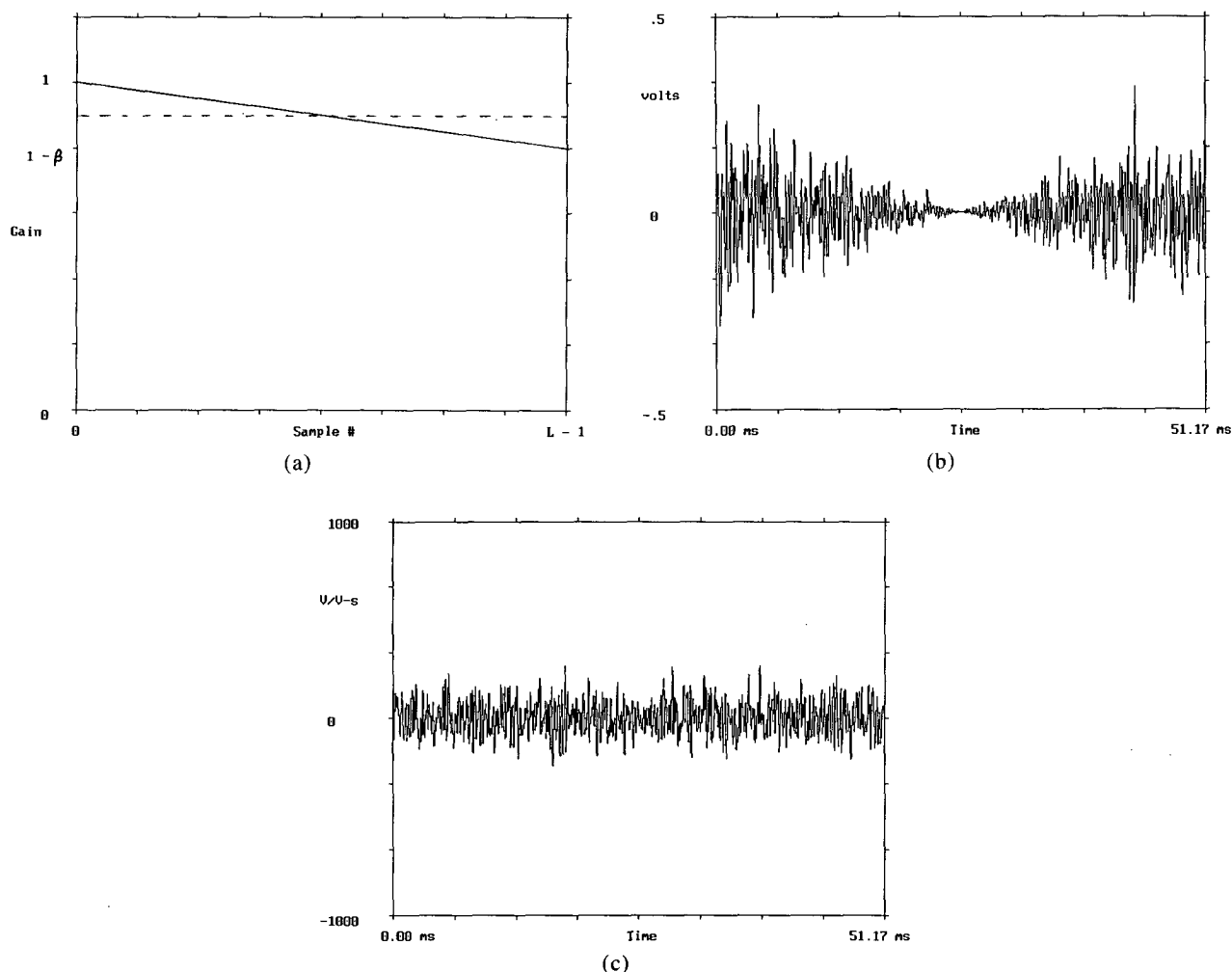


Fig. 4. Effects of slowly varying gain changes during MLS measurement. (a) Linear relative gain change of  $\beta$  over course of one MLS period. (b) Extraneous bowtielike system output, taking undistorted part to refer to average gain of  $1 - \beta/2$ . (c) PIR resulting from (b), indicating that spurious signal acts just like noise contamination.

Suppose that we consider first a slewing for, say, positive edges only. This asymmetrical slewing is a common occurrence, and the results of such distortion are fascinating. A simulation of this is shown in Fig. 5 for a fifth-order MLS of length 31. The MLS is shown in Fig. 5(a), and Fig. 5(b) displays the sequence generated from the positive transitions only of Fig. 5(a). Note that if a positive transition occurs in the original sequence between samples  $n$  and  $n + 1$ , a pulse is placed at sample  $n + 1$  in the derived sequence. Fig. 5(c) shows the normalized cross correlation of Fig. 5(a) and (b), indicating a derivative response at the origin (a doublet) and an isolated inverted peak at delay 18, counting the origin as 0. Fig. 5(d) shows a cross correlation of Fig. 5(a), with the sequence generated by placing negative pulses at the positions of the negative transitions only. Note the derivative response near the origin, and the noninverted peak at delay 18. If the slew distortion is symmetric, then the curves in Fig. 5(a) and (d) will add, resulting in a simple derivative

response at the origin, but the spike at delay 18 is precisely canceled. Slewing that is small relative to the main response will be virtually swamped by it, and only a small derivativelike frequency response aberration occurs. But for *asymmetrical* slewing, the delayed spike gives an image of the impulse response that is well isolated from the main response and could be erroneously interpreted as a delayed reflection, for example, in measuring the impulse response of a room.

What determines the position of this delayed spike? Computer simulations show that for any MLS, the slew-induced peak always occurs at that delay for which the feedback has just complemented its state and the MLS register is then filled with an alternating  $\dots 10101 \dots$  pattern. This is not as strange as it may seem, for the alternating pattern shows maximal activity in a derivative sense. In fact, the sequence produced by placing  $+1$  at the locations of all transitions of either polarity that have just occurred produces a cross correlation with the original MLS, which is a single spike at delay

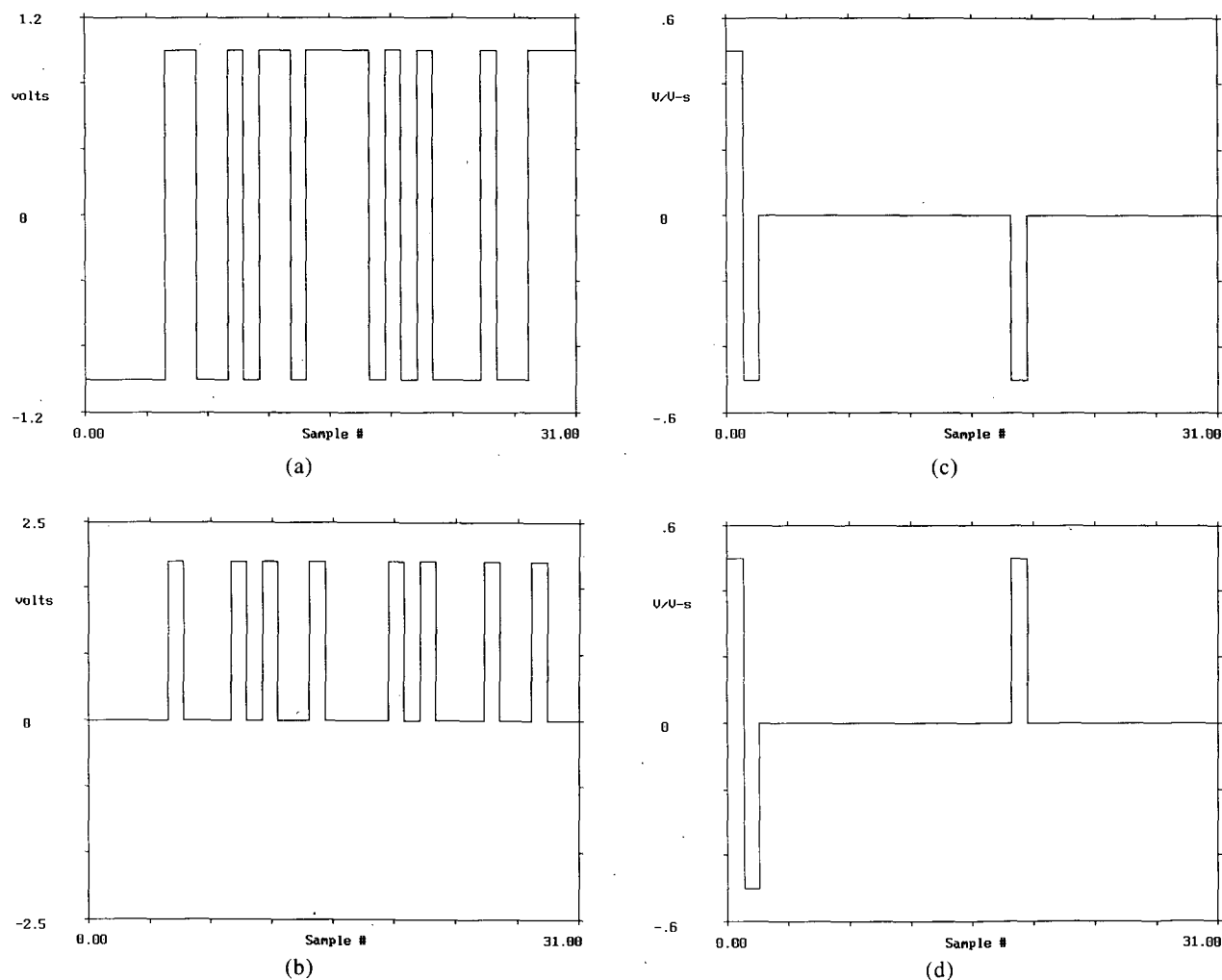


Fig. 5. Effects of slew distortion. (a) Original 31-point signal from 5th-order MLS. (b) Sequence produced by only positive transitions of (a). (c) PIR resulting from cross correlation with (a). Note response at sample 0 is a derivative, but isolated inverted impulse at delay 18 results in image of original impulse response at this delay. (d) PIR resulting from error signal made up of only negative transitions of (a). If slewing distortion is precisely symmetrical for negative and positive transitions, net effect is sum of (c) and (d) so that only a derivative error component occurs at position of undistorted PIR peak. However, a common occurrence with a sharp-edged signal such as an unfiltered MLS is asymmetrical slewing, and then a confounding image will occur at some delay in PIR, as indicated in Table 1.

18, and represents essentially the curve of Fig. 5(c) with Fig. 5(d) subtracted. This sequence then must be identical to the original sequence, but delayed. Thus the sequence generated by the transitions of an MLS is also an MLS.

It is not known how to predict with a simple mathematical approach the position of the slew peak. Computer simulation can be used to compute the position of this peak, given the MLS order and the feedback taps. Table 1 shows the sample positions of the slew-induced peak relative to the impulse at bin 0 for a series of orders and taps. Included are some of the combinations used in commercially available MLS systems. The symmetry of the sequences allows others to be simply predicted from the entries in the table. For example, if a slew peak occurs at bin  $S$  for MLS order  $M$  and taps at  $M, T_1, T_2, T_3, \dots$  ( $T_2, T_3, \dots$  may not exist of course), then the slew peak for MLS order  $M$  and taps  $M, M - T_1, M - T_2, M - T_3$  occurs at bin  $2^M - S$ , since this causes a time reversal of the sequence. Thus, for example, the 16th-order sequence with taps at 16, 5, 3, 2 gives a slew peak at bin 61481, whereas when the taps are 16, 11, 13, 14, the slew peak is at  $2^{16} - 61481 = 4055$ .

Shown in the table are some sequences with 6, 8, and 10 taps. These sequences are excerpted from a study by Tomlinson and Galvin [14], which shows that having more taps generates sequences which show less skewing of the PDF when low-pass filtered.

It is probably best that the spurious delayed spike should occur near the middle of the repetition period, being then most removed from the main response in a periodic sense. The feedback taps can be chosen by simulations to arrange an acceptable spike position. For MLS registers with only two taps, one of course coming from the last register, the second tap should not be chosen from either the first position or the second from last shift position. Such generators create the  $\dots 10101 \dots$  alternating state just before or after the all 1s state. Hence the spurious spike is removed from the main one by only  $r$  samples, where  $r$  is the order of the MLS register.

The author remembers well an MLS reverberation measurement at a theater in Toronto in which a sharp "echo" occurred at an equivalent path delay of about 120 m. The sampling rate was 10 kHz, and an order 14 MLS was used with feedback taps 14, 13, 12, 2. The "echo" disappeared upon reducing the drive to the

Table 1. MLS parameters and associated slew peaks.

Order	Length	Taps	Slew Peak
2	3	2, 1	2
3	7	3, 1	3
4	15	4, 1	4
5	31	5, 2	18
6	63	6, 1	6
7	127	7, 1	7
8	255	8, 6, 5, 1	197
9	511	9, 4	130
10	1023	10, 7	947
11	2047	11, 2	1029
12	4095	12, 11, 10, 2	2368
12	4095	12, 7, 4, 3	4032
13	8191	13, 4, 3, 1	934
13	8191	13, 12, 11, 9, 6, 5, 2, 1	6135
14	16383	14, 13, 12, 2	3515
14	16383	14, 12, 11, 1	7558
14	16383	14, 12, 10, 9, 7, 5, 3, 1	13512
15	32767	15, 14	32753
15	32767	15, 11	8189
15	32767	15, 8	28673
15	32767	15, 12, 11, 8, 7, 6, 4, 2	11562
16	65535	16, 5, 3, 2	61481
16	65535	16, 12, 11, 10, 7, 4, 3, 2	41583
17	131071	17, 3	9300
17	131071	17, 14, 13, 9	130155
17	131071	17, 14, 11, 9, 6, 5	98321
17	131071	17, 15, 13, 11, 10, 9, 8, 4, 2, 1	15045
18	262141	18, 7	209765
19	524287	19, 6, 5, 1	33831
20	1048575	20, 3	212012
21	2097151	21, 2	1048586
22	4194303	22, 1	22
23	8388607	23, 5	6723362
24	16777215	24, 4, 3, 1	5114717
25	33554431	25, 3	1364812
26	67108863	26, 8, 7, 1	16942295
27	134217727	27, 8, 7, 1	33677214
28	268435455	28, 3	117095305
29	536870911	29, 2	268435470
30	1073741823	30, 16, 15, 1	509339714
31	2147483647	31, 3	262143
32	4294967295	32, 28, 27, 1	165852194

power amplifiers by 10 dB. Hence we concluded that slew-induced distortion was responsible, and indeed the delay agreed with a later computer simulation. As an effective countermeasure against slew-induced distortion it would be advisable to filter the MLS signal to the band of interest, thereby dulling the edges. Any active circuits in the filter must be designed to avoid slewing.

On the positive side, by monitoring the PIR in the vicinity of the expected delay for slewing images, one can guard against problems from slewing.

If an MLS is passed through a low-pass filter with cutoff frequency set somewhat below half the sampling frequency, the excitation has moderated slewing that is not the same for each transition. In this circumstance slew limiting might occur on just some transitions, not on each one, and then the result in the PIR would be a series of spikes, not just the isolated one shown in the simulations of Table 1.

## 6 A NEW TOTAL DISTORTION MEASURE

We have seen that distortion produces spurs in the PIR that are spread in more or less random fashion. Most systems being tested, however, have true impulse responses that decay to negligible values if an appropriate MLS repetition period is chosen. Hence the occurrence of late-time artifacts, in a region where the PIR should be negligible, indicates the presence of distortion, and the level of these artifacts relative to the linear portion of the PIR gives a measure of the fractional distortion under MLS excitation.

An MLS, however, has a perfectly white spectrum (except for the zero-hold correction and any low-pass filters in the MLS output) so the excitation is not very representative of real audio, just as it could be argued that sinusoids are also not very similar to a real audio signal. Consider then a particular spectrum that we might desire in order to simulate audio more realistically. It might have a peak at frequencies around 200–400 Hz, a gentle rolloff at middle frequencies, and a 12- or 18-dB per octave rolloff at high frequencies. An analog or digital filter designed to give such a spectrum when fed with a white MLS would impose its own impulse response on the audio system under test in a convolutional sense, yet the net PIR would still decay sufficiently if an appropriately long MLS repetition period were chosen.

Thus we can construct a system whose excitation has an appropriate audio spectrum (but not necessarily the correct temporal response) and the distortion of this system will again produce spurs throughout the PIR. By inspection we can isolate an area of the PIR during which the linear response is essentially zero, and thus estimate the average energy of the spurs. Then we can assume that the same level of spurs occurs even in those regions of the PIR that are dominated by linear contributions. Hence by simple extrapolation we can determine the total distortion energy, and by subtraction from the total energy, derive the

total linear energy.

In this way the total distortion fraction can be evaluated for a system excited by any desired spectrum. In addition the spectrum of the distortion can be estimated if a sufficiently representative portion of it is available without "contamination" from the linear part. The best way to achieve such conditions is to use MLS repetition periods much longer than the length of the impulse response. This can always be done in principle. Thus it seems that with a sufficiently long MLS, both the linear transfer function and the distortion energy can be determined. The linear portion, however, may not be the same as that measured under different signal levels.

Another valuable use of the time-domain separation of linear and nonlinear effects for MLS systems is the determination of rumble and buzz in electroacoustic transducers. Other methods using tones and FFT analysis [16] have been investigated, but the MLS approach offers wide-band excitation which may in some cases be much better than signals that are less spectrally dense.

## 7 ANOTHER LOOK AT DISTORTION IMMUNITY

If the distortion component in the PIR is uniformly distributed, its contribution can be largely removed from any analysis involving energy integrals, such as reverberation plots, or other room acoustic parameters, such as clarity or center time. But low-order distortion is not very uniformly distributed, and in fact it results in spurious images of the linear impulse response, as shown in Fig. 2. Rather than being a detriment, however, this spikelike component can be easily identified if the same measurement is repeated with a different MLS sequence of the same order. The data of Fig. 2(c) and (g) show this quite well.

Hence a new possibility occurs. By comparing two or more measurements on the same system with MLSs of the same order but different feedback taps, the distortion spikes can be identified and removed by appropriate editing. The resulting PIR is then a better representation of the linear component of the impulse response of the system. Such nonlinear processing can be automated in a program, and then results in a distortion-immunity increase for low-order distortion, for example.

## 8 CONCLUSION

MLS measuring systems behave in unusual ways when nonlinearities occur in the DUT. We have shown by measurements and simulations how these effects are manifest. The presence of distortion can be easily ascertained, and some analyses have been presented which allow extraction of certain interesting aspects.

## 9 ACKNOWLEDGMENT

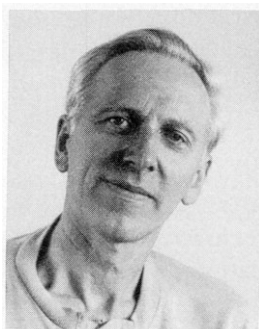
This work has been supported by the Natural Sciences and Engineering Research Council of Canada. The author wishes to thank Chris Dunn for stimulating dis-

cussions during a four-month stay at the University of Essex, England.

## 10 REFERENCES

- [1] R. C. Heyser, "Acoustical Measurements by Time Delay Spectrometry," *J. Audio Eng. Soc.*, vol. 15, pp. 370–382 (1967 Oct.).
- [2] K. Jebelian, "A Real-Time Digital Approach to Time Delay Spectrometry," presented at 89th Convention of the Audio Engineering Society, *J. Audio Eng. Soc. (Abstracts)*, vol. 38, p. 874 (1990 Nov.), preprint 2988.
- [3] M. A. Poletti, "Linearly Swept Frequency Measurements, Time-Delay Spectrometry, and the Wigner Distribution," *J. Audio Eng. Soc.*, vol. 36, pp. 457–468 (1988 June).
- [4] M. A. Poletti, "The Application of Linearly Swept Frequency Measurements," *J. Acoust. Soc. Am.*, vol. 84, pp. 599–610 (1988 Aug.).
- [5] J. Vanderkooy, "Another Approach to Time-Delay Spectrometry," *J. Audio Eng. Soc.*, vol. 34, pp. 523–538 (1986 July/Aug.).
- [6] H. Biering, O. Z. Pedersen, and J. Vanderkooy, "Comment on 'Another Approach to Time-Delay Spectrometry,'" and Author's Reply, *J. Audio Eng. Soc. (Letters to the Editor)*, vol. 35, pp. 145–146 (1987 Mar.).
- [7] J. M. Berman and L. R. Fincham, "The Application of Digital Techniques to the Measurement of Loudspeakers," *J. Audio Eng. Soc.*, vol. 25, pp. 370–384 (1977 June).
- [8] L. R. Fincham, "Refinements in the Impulse Testing of Loudspeakers," *J. Audio Eng. Soc.*, vol. 33, pp. 133–140 (1985 Mar.).
- [9] M. R. Schroeder, "Integrated-Impulse Method Measuring Sound Decay without Using Impulses," *J. Acoust. Soc. Am.*, vol. 66, pp. 497–500 (1979 Aug.).
- [10] H. Alrultz, as described in Y. Ando, *Concert Hall Acoustics* (Springer, New York, 1985), pp. 103–109.
- [11] J. Borish and J. B. Angell, "An Efficient Algorithm for Measuring the Impulse Response Using Pseudorandom Noise," *J. Audio Eng. Soc.*, vol. 31, pp. 478–488 (1983 July/Aug.).
- [12] D. D. Rife and J. Vanderkooy, "Transfer-Function Measurements with Maximum-Length Sequences," *J. Audio Eng. Soc.*, vol. 37, pp. 419–444 (1989 June).
- [13] C. Dunn and M. O. Hawksford, "Distortion Immunity of MLS-Derived Impulse Response Measurements," *J. Audio Eng. Soc.*, vol. 41, pp. 314–335 (1993 May).
- [14] G. H. Tomlinson and P. Galvin, "Analysis of Skewing in Amplitude Distributions of Filtered *M* Sequences," *Proc. IEEE*, vol. 121, pp. 1475–1479 (1974 Dec.).
- [15] S. W. Golomb, *Shift Register Sequences* (Aegean Park Press, Laguna Hills, CA, 1982).
- [16] G. G. Groeper, M. A. Blanchard, T. Brummett, and J. Bailey, "A Reliable Method of Loudspeaker Rub and Buzz Testing Using Automated FFT Response and Distortion Techniques," presented at 91st Convention of the Audio Engineering Society, *J. Audio Eng. Soc. (Abstracts)*, vol. 39, p. 1002 (1991 Dec.), preprint 3161.

## THE AUTHOR



John Vanderkooy was born in The Netherlands in 1941, but received all of his education in Canada, with a B.Eng. degree in engineering physics in 1963 and a Ph.D. in physics in 1967, both from McMaster University in Hamilton, Ontario. For some years he followed his doctoral interests in low-temperature physics of metals at the University of Waterloo, where he is currently a professor of physics. However, since the late 1970s, his research interests have been mainly in audio and electroacoustics.

A fellow of the AES and a member of the IEEE, Dr.

Vanderkooy has contributed a variety of papers at conventions and to the *Journal*. Together with his colleague Stanley Lipshitz and a number of graduate and undergraduate students, they form the Audio Research Group at the University of Waterloo.

Dr. Vanderkooy's current interests are digital audio signal processing, measurement of transfer functions with maximum-length sequences, transducers, diffraction of loudspeaker cabinet edges, and most recently sub-surface analysis techniques using maximum-length sequences.